

NRL Report 7296

The Analysis of Internally Redundant  
Structural Cable Arrays

Richard A. Skop and George J. O'Hara

Applied Mechanics Branch  
Ocean Technology Division

September 1, 1971

Approved for public release; distribution  
unlimited

## DOCUMENT CONTROL DATA - R &amp; D

(Security classification of title, body of abstract and indexing annotation must be entered when the overall report is classified)

1. ORIGINATING ACTIVITY (Corporate author) Naval Research Laboratory Washington, D.C. 20390		2a. REPORT SECURITY CLASSIFICATION Unclassified	
		2b. GROUP	
3. REPORT TITLE  THE ANALYSIS OF INTERNALLY REDUNDANT STRUCTURAL CABLE ARRAYS			
4. DESCRIPTIVE NOTES (Type of report and inclusive dates) Interim report on one phase of the NRL Problem; work is continuing on other phases			
5. AUTHOR(S) (First name, middle initial, last name)  Richard A. Skop and George J. O'Hara			
6. REPORT DATE September 1, 1971		7a. TOTAL NO. OF PAGES 34	7b. NO. OF REFS 5
8a. CONTRACT OR GRANT NO. NRL Problem F02-24		9a. ORIGINATOR'S REPORT NUMBER(S)  NRL Report 7296	
b. PROJECT NO. RR 009-03-45-5807		9b. OTHER REPORT NO(S) (Any other numbers that may be assigned this report)	
c.			
d.			
10. DISTRIBUTION STATEMENT  Approved for public release; distribution unlimited			
11. SUPPLEMENTARY NOTES		12. SPONSORING MILITARY ACTIVITY Department of the Navy (Office of Naval Research), Arlington, Virginia 22217	
13. ABSTRACT A method is presented for determining the tensions in, and equilibrium configuration of, internally redundant structural cable arrays. The method has applications to suspension bridges, structural nets, and moorings. Cable stretch is included in the formulation, and arbitrary strain-tension relations are permitted. An iterative solution, that does not require the calculation of slopes or derivatives, is generated for varying the unknown redundant reactions. Global convergence of the iteration to the correct reactions (and consequently to the correct equilibrium configuration of the array) from any set of initially guessed reactions is insured. The rapidity of this convergence is demonstrated by several numerical examples. Although the basic solution assumes external loads that are independent of the array configuration, a combination of the method with the mathematical technique of successive approximations allows configuration-dependent loadings to also be treated. This combined technique is described.			

14. KEY WORDS	LINK A		LINK B		LINK C	
	ROLE	WT	ROLE	WT	ROLE	WT
Cables Cable arrays Cable structure analysis Cable structure design Moorings Suspension bridges Structural nets Structural analysis Nonlinear structural analysis Consistent deformation theory Imaginary reactions						

## CONTENTS

Abstract	ii
Problem Status	ii
Authorization	ii
INTRODUCTION	1
DESCRIPTION OF THE SYSTEM	1
ANALYSIS OF THE SYSTEM	2
Imaging in Air	2
Meaning of Resolution to the Observer	5
Addition of Intensifiers to the Image Dissector	9
UNDERWATER APPLICATIONS	13
Light Transmission in the Sea	13
Analysis	13
SUMMARY	16
ACKNOWLEDGMENT	16
REFERENCES	16

## ABSTRACT

A scanned-laser active imaging system employing a synchronously scanned image-dissector detector was analyzed from the standpoint of how much resolution would be available to an observer viewing a CRT display. Graphical results are given of the system performance in atmospheric and underwater environments as well as of the effects of laser power, wavelength, and the addition of image intensifiers to the receiving system. The novelty of the analysis is that it directly predicts the detection performance of the human observer when aided by a scanned-laser active imaging system. The performance of such a system compares favorably with range-gated active imaging systems.

## PROBLEM STATUS

This work was begun while the author was employed part-time at the Westinghouse Defense and Space Center and was continued while at NRL. It has been completed in the belief that it will assist the Navy's research and development program and is being issued as an interim report on an NRL Problem.

## AUTHORIZATION

NRL Problem N01-24  
Project RR 104-03-41

Manuscript submitted April 7, 1971.

# APPLICATION OF A SCANNED-LASER ACTIVE IMAGING SYSTEM TO ATMOSPHERIC AND UNDERWATER VIEWING ENVIRONMENTS

## INTRODUCTION

Man wants to see what is in the dark. He has developed candles, lanterns, street lights, flashlights, and automobile headlights as active sources to light up the darkness. Recently he has achieved impressive results with passive vision-aiding systems such as low-light-level television and image-intensifier chains. To augment the illumination when insufficient for these passive devices, active systems have been proposed that will use lasers as light sources.

All active systems are limited in their performance by backscatter from the atmosphere. The automobile headlight in fog is a familiar example of the increased imaging difficulty caused by backscatter. One way to reduce the effect of backscatter is to use a pulsed laser and a receiver that can be gated on only when the return from the desired target arrives at the receiver. This type of system has been analyzed by Steingold and Strauch (1) without considering laser sources specifically. Another somewhat novel system is possible, however, which also eliminates backscatter. In this system a CW laser is scanned to illuminate a screen in synchronism with the scanning of an image dissector used as a receiver to present a cathode-ray-tube (CRT) display. This system appears to have limitations similar to the gated system with the exception that first-order backscatter is inherently eliminated for the scanned system, whereas it can only be approached in the gated system.

Since the only meaningful performance criterion for comparison of display systems is the information presented to a display observer, it would be helpful if this analysis of a scanned-laser active imaging system would present data relative to the observer. Following the method of Rosell (2), the scanned system has been analyzed. Theoretical curves have been derived of observer display resolution vs range for various scene contrasts, visibilities, and laser powers and wavelengths.

## DESCRIPTION OF THE SYSTEM

A general raster scanning system is shown in Fig. 1. This system could apply to an airplane observing earth terrain, a satellite observing a distant planet, or an aquanaut or remote observer observing the bottom of the ocean. Both the laser illumination and the dissector receiving aperture are scanned over an angle  $\alpha$ . For simplicity it is assumed that all target points within the angle are at a distance  $r$  from the illuminator/receiver system. Also,  $\theta_1$  is defined as the half angle of the receiver system, and  $\theta_2$  is defined as the half angle of the laser beam. This beam will be assumed small and adjustable with optics to fit the receiver's active area at any distance. The receiver diameter will be denoted by  $Y_1$ , and the initial diameter of the laser beam will be denoted by  $Y_2$ . The transmitted laser power will be called  $w$ .

Note: This report represents work that was done in part while the author was affiliated with the Westinghouse Electric Corp., Defense and Space Center, Baltimore, Md., and which has since been expanded to include the undersea environment.

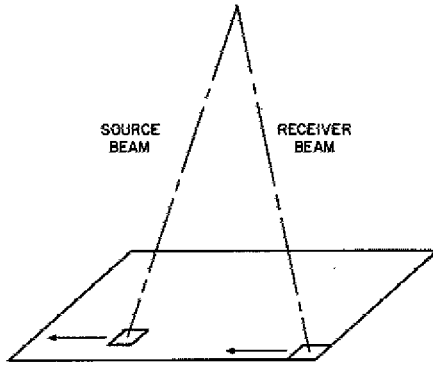


Fig. 1 - Geometry showing source beam (laser) and receiver beam (image-dissector active area). Due to the finite propagation time, the receiver never looks into the (first order) backscatter of the source beam.

The novelty of this system can be appreciated by considering Fig. 1. Due to the propagation time required for the laser beam to travel the distance  $2r$ , a scanned beam directed at a spot will return to the receiver  $2r/c$  sec later. The receiver beam, if pointed at the initial spot  $2r/c$  sec after transmission, will receive the photons reflected from that spot. The illuminating beam, for most practical systems, will be far away from the point being observed by the receiver; therefore, no backscatter from the laser will enter the receiver. By adjustment of scanning speed, separation of illuminator and receiver, or reduction of the illuminator/receiver angle, almost any system can be made free from first-order backscatter.

#### ANALYSIS OF THE SYSTEM

##### Imaging in Air

The receiver and source diameters at a distance  $r$  are defined as

$$y_1 = Y_1 + r \tan \theta_1 \quad (1)$$

and

$$y_2 = Y_2 + r \tan \theta_2 . \quad (2)$$

The transmitting angle can be made equal to the active angle of the receiver by using the equation

$$\theta_2 = \theta_1 + \frac{Y_1 - Y_2}{r} . \quad (3)$$

This makes the illuminated area equal to the actively viewed area. The power density supplied to this area is given by

$$\text{power density} = \frac{We^{-ar}}{\pi y_1^2} , \quad (4)$$

where  $a$ , the loss coefficient in air, is given by

$$a = \left( \frac{3.91 \times 10^{-3}}{V} \right) \left( \frac{550}{\lambda} \right) 0.585V^{1/3} . \quad (5)$$

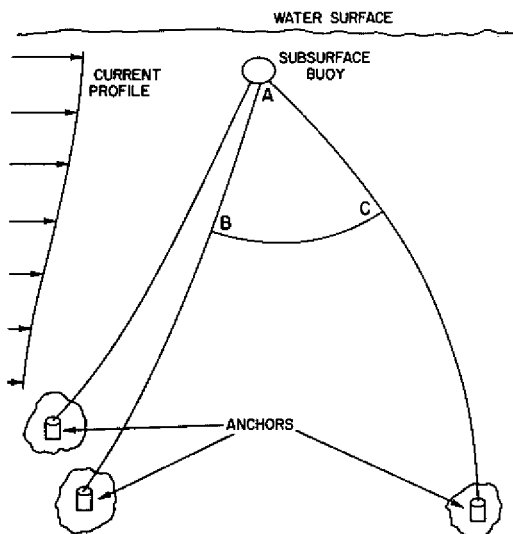


Fig. 1 - Example of a subsurface moor which cannot be analyzed by the Method of Imaginary Reactions because of the internal loop of cable ABC

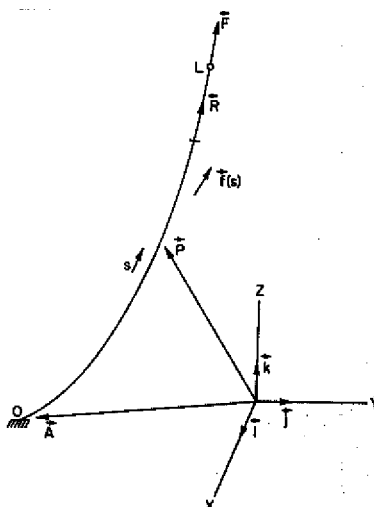


Fig. 2 - Equilibrium configuration of a loaded cable

and the position of a point on the cable is given by the vector  $P$  with components

$$P = xi + yj + zk .$$

The measure of *unstressed* arc length along the cable is denoted by  $s$ , which increases from zero to the total *unstressed* length of cable  $L$  in the indicated direction. The load on the cable per unit of *unstressed* arc length is defined by the vector  $f(s)$ . In addition a vector point force  $F$  acts at the free end of the cable.

The internal reaction of the cable to this system of external loads is represented by the resultant force vector  $R$  with components

$$R = R_x i + R_y j + R_z k .$$

Since the cable is assumed to be perfectly flexible, its equilibrium direction is parallel to  $R$ , and its equilibrium tension  $T$  is equal to the magnitude of  $R$ . Elementary considerations of static force balance then yield the resultant force vector as

$$R(s) = F - \int_L^s f(\xi) d\xi \tag{1a}$$

and consequently the tension as

$$T(s) = |R(s)| = (R \cdot R)^{1/2} = (R_x^2 + R_y^2 + R_z^2)^{1/2} . \tag{1b}$$

The strain  $\epsilon$  in the cable can now be obtained from the constitutive equation, which in its most general static form has the functional relationship

$$\epsilon = \epsilon(T, s) . \quad (1c)$$

This equation is quite arbitrary; that is, the cable is not restricted to being, for example, inextensible ( $\epsilon = 0$ ) or linear ( $\epsilon \propto T$ ). The dependence of the constitutive relation on the unstressed arc length  $s$  simply indicates that the cable can be composed of various sub-cables of different sizes and/or materials.

Finally, on taking into account the equilibrium direction and extension, the static configuration of the cable in Fig. 2 is found by quadrature of the formula

$$P(s) = A + \int_0^s [1 + \epsilon(\xi)] [R(\xi)/T(\xi)] d\xi . \quad (1d)$$

Equations (1a) through (1d) form the basis for evaluating the equilibrium configuration of any cable array which is analyzed by using either the Method of Imaginary Reactions or the Extended Method.

## THE EXTENDED METHOD

### Basic Concepts

Consider now the problem of determining the equilibrium configuration of the loaded, internally redundant cable array shown in Fig. 3. The cables forming the array are designated by the numbers 1, 2, etc., as indicated in the figure, and quantities associated with a particular cable are denoted by a subscript corresponding to that cable number. Thus the vector  $A_3$  denotes the anchor location of cable 3,  $s_2$  denotes the measure of unstressed arc length along cable 2, and  $f_4(s_4)$  represents the load per unit of unstressed arc length on cable 4.

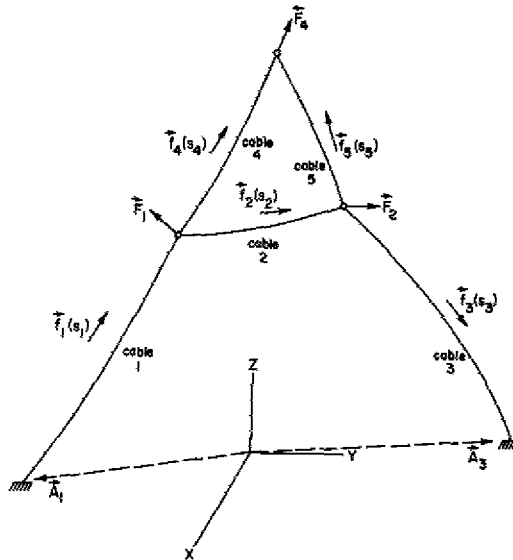


Fig. 3 - Equilibrium configuration of a loaded, internally redundant cable array

The analysis of this array by the Method of Imaginary Reactions would proceed by releasing cable 3 from its anchor and replacing the effect of the anchor by a guessed, or imaginary, reaction  $I_3$  acting at the end of cable 3. However, because of the internal loop formed by cables 2, 4, and 5, the release of this redundant anchor is insufficient to permit the determination of the equilibrium configuration of the resulting array.

Suppose though that, besides releasing the redundant anchor, a cut is also made somewhere within the internal loop of cable — for example, above the junction of cables 5 and 3. This cut creates a statically determinant array; and, if the forces of internal constraint released by the cut are replaced by a guessed reaction  $I_5$  acting at the end of cable 5, the loads on the resulting array are as depicted in Fig. 4a. The additional reaction  $-I_5$ , which must be imposed at the junction of cables 2 and 3, follows as a direct consequence of Newton's third law.

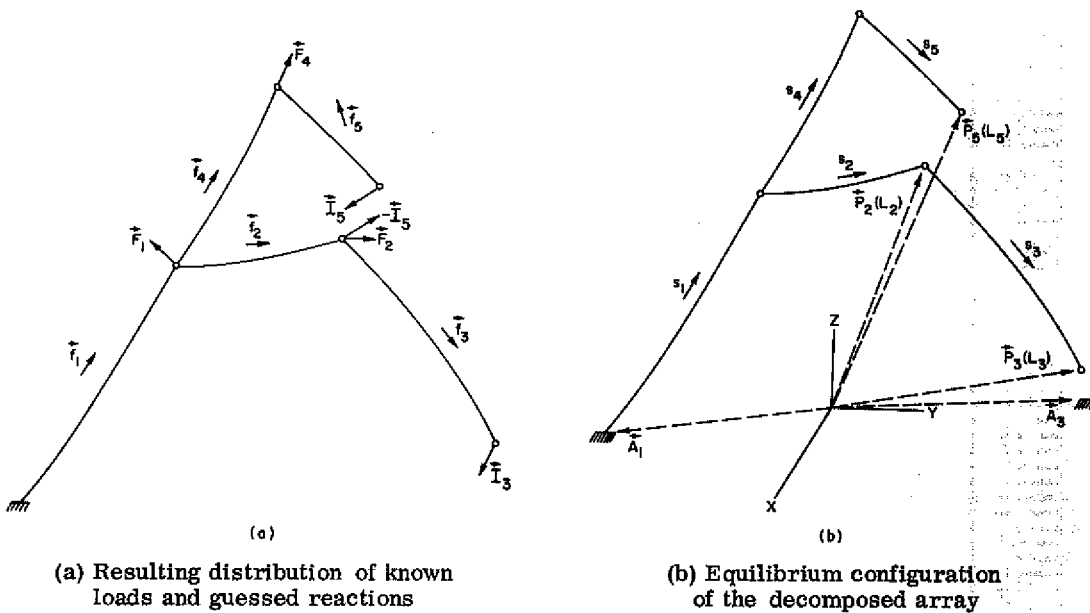


Fig. 4 - Decomposition of the internally redundant cable array shown in Fig. 3 as prescribed by the Extended Method of Imaginary Reactions

If now the directions of increasing arc length (from 0 to  $L_n$ ) are assigned as indicated in Fig. 4b, then the resultant force vector at any point in the decomposed array can be obtained by combining Eq. (1a) with a balance of forces at the cable junctions. This gives

$$R_5(s_5) = I_5 - \int_{L_5}^{s_5} f_5(\xi) d\xi, \tag{2a}$$

$$R_4(s_4) = F_4 + R_5(0) - \int_{L_4}^{s_4} f_4(\xi) d\xi, \tag{2b}$$

$$\mathbf{R}_3(s_3) = \mathbf{I}_3 - \int_{L_3}^{s_3} \mathbf{f}_3(\xi) d\xi, \quad (2c)$$

$$\mathbf{R}_2(s_2) = \mathbf{F}_2 - \mathbf{I}_5 + \mathbf{R}_3(0) - \int_{L_2}^{s_2} \mathbf{f}_2(\xi) d\xi, \quad (2d)$$

$$\mathbf{R}_1(s_1) = \mathbf{F}_1 + \mathbf{R}_2(0) + \mathbf{R}_4(0) - \int_{L_1}^{s_1} \mathbf{f}_1(\xi) d\xi. \quad (2e)$$

The tensions and strains in each cable are calculated from Eqs. (1b) and (1c) respectively; finally, the equilibrium configuration of the decomposed array (Fig. 4b) is determined from Eq. (1d) as

$$\mathbf{P}_1(s_1) = \mathbf{A}_1 + \int_0^{s_1} [1 + \varepsilon_1(\xi)] [\mathbf{R}_1(\xi)/T_1(\xi)] d\xi, \quad (3a)$$

$$\mathbf{P}_2(s_2) = \mathbf{P}_1(L_1) + \int_0^{s_2} [1 + \varepsilon_2(\xi)] [\mathbf{R}_2(\xi)/T_2(\xi)] d\xi, \quad (3b)$$

$$\mathbf{P}_3(s_3) = \mathbf{P}_2(L_2) + \int_0^{s_3} [1 + \varepsilon_3(\xi)] [\mathbf{R}_3(\xi)/T_3(\xi)] d\xi, \quad (3c)$$

$$\mathbf{P}_4(s_4) = \mathbf{P}_1(L_1) + \int_0^{s_4} [1 + \varepsilon_4(\xi)] [\mathbf{R}_4(\xi)/T_4(\xi)] d\xi, \quad (3d)$$

$$\mathbf{P}_5(s_5) = \mathbf{P}_4(L_4) + \int_0^{s_5} [1 + \varepsilon_5(\xi)] [\mathbf{R}_5(\xi)/T_5(\xi)] d\xi. \quad (3e)$$

In general, for an arbitrary set of guessed reactions the equilibrium configuration calculated for the decomposed array does not satisfy the geometric constraints on the original array. That is,  $\mathbf{P}_3(L_3) \neq \mathbf{A}_3$  and  $\mathbf{P}_5(L_5) \neq \mathbf{P}_2(L_2)$ . As a measure of the error between the calculated and actual configurations, the positive definite error function  $E$  is defined as

$$E = \left\{ |\mathbf{A}_3 - \mathbf{P}_3(L_3)|^2 + |\mathbf{P}_2(L_2) - \mathbf{P}_5(L_5)|^2 \right\}^{1/2} \quad (4a)$$

or in expanded form as

$$E = \left\{ [a_3 - x_3(L_3)]^2 + [b_3 - y_3(L_3)]^2 + [c_3 - z_3(L_3)]^2 + [x_2(L_2) - x_5(L_5)]^2 + [y_2(L_2) - y_5(L_5)]^2 + [z_2(L_2) - z_5(L_5)]^2 \right\}^{1/2}. \quad (4b)$$

Since  $E$  is the square root of the sum of the squares of the individual coordinate errors,  $E$  vanishes identically when and only when the true equilibrium configuration has been obtained.

The question then arises: Can the actual reactions, which make  $E$  identically zero, be found so that the equilibrium configuration of the array can be determined without recourse to solving the full, nonlinear, force balance-geometric constraint equations of the system? The Extended Method of Imaginary Reactions answers this question affirmatively.

Let the additional forces  $\Delta I_3$  and  $\Delta I_5$  be applied at the ends of cables 3 and 5 respectively. (Simultaneously the additional force  $-\Delta I_5$  must be applied at the junction of cables 2 and 3, so that Newton's third law remains satisfied.) The values of these additive forces are given by

$$\Delta I_3 = (\delta/E)[A_3 - P_3(L_3)] \quad (5a)$$

and

$$\Delta I_5 = (\delta/E)[P_2(L_2) - P_5(L_5)] \quad (5b)$$

The force  $\Delta I_3$  is taken to act in the direction from the end of cable 3 to its required point of anchorage  $A_3$ , and the force  $\Delta I_5$  is taken to act in the direction from the end of cable 5 to its required point of junction with cables 2 and 3.

The symbol  $\delta$  denotes a *positive* number, having the dimension of force, yet to be determined. In essence, it is a convergence parameter used to choose the magnitude of the additive forces in a manner such that the decomposed array approaches the correct equilibrium position. It is important to recognize that, since the ratios  $[a_3 - x_3(L_3)]/E$ ,  $[x_2(L_2) - x_5(L_5)]/E$ , etc. are of bounded variation (between -1 and +1), the convergence parameter  $\delta$  must approach zero as  $E$  becomes small.

#### Iterative Procedure

The full concept of the solution, with reference to the array in Fig. 3, can now be laid out:

1. Release the redundant anchor  $A_3$  and replace its effect by an imaginary reaction  $I_3$  acting at the end of cable 3.
2. Make a cut somewhere within the internal loop of cable — for example, above the junction of cables 5 and 3. Replace the internal forces released by this cut by an imaginary reaction  $I_5$  acting at one side of the cut and an equilibrating reaction  $-I_5$  acting at the other side.
3. Choose initial values for  $I_3$  and  $I_5$ . Any values consistent with the static stability of the loaded array are acceptable.
4. The structure is now statically determinant (Fig. 4). Calculate the equilibrium configuration and from this the quantities  $A_3 - P_3(L_3)$ ,  $P_2(L_2) - P_5(L_5)$ , and  $E$ .
5. Choose an initial value of  $\delta$  to find candidates for  $\Delta I_3$  and  $\Delta I_5$ . The value of  $\delta$  can be chosen large, since it will of necessity become smaller as the solution proceeds step by step. In fact, at first choose  $\delta$  to be the order of magnitude of the guessed reactions.
6. Calculate the new equilibrium configuration of the array when the candidate reactions  $I_3' = I_3 + \Delta I_3$  and  $I_5' = I_5 + \Delta I_5$  are applied at the ends of cables 3 and 5 respectively. (The candidate reaction  $-I_5'$  must simultaneously be applied at the junction of cables 2 and 3.)

7. If  $E'$ , the new measure of error, is less than  $E$ , the old measure, then a successful step has been made. In this event, begin again from *this new configuration* by changing the retained values of  $I_3$ ,  $I_5$ ,  $A_3 - P_3(L_3)$ ,  $P_2(L_2) - P_5(L_5)$ , and  $E$  to those values calculated from this *new* configuration. Retain the same value of  $\delta$  and proceed with another iteration by finding the new  $\Delta I$ 's and the corresponding equilibrium configuration.

8. Possibly on the first step, but certainly on some subsequent step, the candidate  $E'$  will be found to be greater than or equal to  $E$  of the previous step. Then  $\delta$  is too large. The candidate values should be rejected and the previous ones retained by returning to the former equilibrium configuration of  $E < E'$ .

9. Reduce  $\delta$ ; halving is suggested. Proceed from the last acceptable configuration until again a candidate  $E'$  is found to succeed.

10. This iterative process continues until the error function  $E$  becomes as small as desired.

Since  $E$  vanishes only at the real rather than at an imaginary array configuration, a solution of the entire problem has been found by considering only statically determinant arrays. There is no need to be particular in the choice of  $\delta$ : choose an initial value, let it remain constant until the candidate  $E' \geq E$ , and then halve it.

It is important to note that the Extended Method of Imaginary Reactions is globally convergent. That is, the iterative process converges to  $E = 0$  from any set of initially guessed reactions consistent with the static stability of the system. Proofs of the existence of a positive  $\delta$  at each iterative step, of the convergence of  $E$  to zero, and of the uniqueness of the calculated reactions are given in the first section of the Appendix.

#### Numerical Example I

To illustrate the convergence and the simplicity of the Extended Method of Imaginary Reactions, consider the array acted on by the two-dimensional system of point loads shown in Fig. 5a. The unstressed cable lengths and constitutive relations are as indicated on the diagram. Cables 1 and 3 are inextensible, cables 4 and 5 are linear, and cable 2 is nonlinear. When the array is decomposed as illustrated in Fig. 5b and the imaginary reactions  $I_3$  and  $I_5$  are applied, the resultant force in each cable is readily calculated from Eq. (2) as

$$R_5(s_5) = I_5 ,$$

$$R_4(s_4) = F_4 + R_5(0) = -4.797016 \, i + 6.148782 \, k + I_5 ,$$

$$R_3(s_3) = I_3 ,$$

$$R_2(s_2) = F_2 - I_5 + R_3(0) = 3.147936 \, i - I_5 + I_3 ,$$

$$R_1(s_1) = F_1 + R_2(0) + R_4(0) = -4.010032 \, i + 6.148782 \, k + I_3 .$$

The tensions are obtained from Eq. (1b) as

$$T_n(s_n) = \left[ R_{nX}^2 + R_{nZ}^2 \right]^{1/2} ,$$

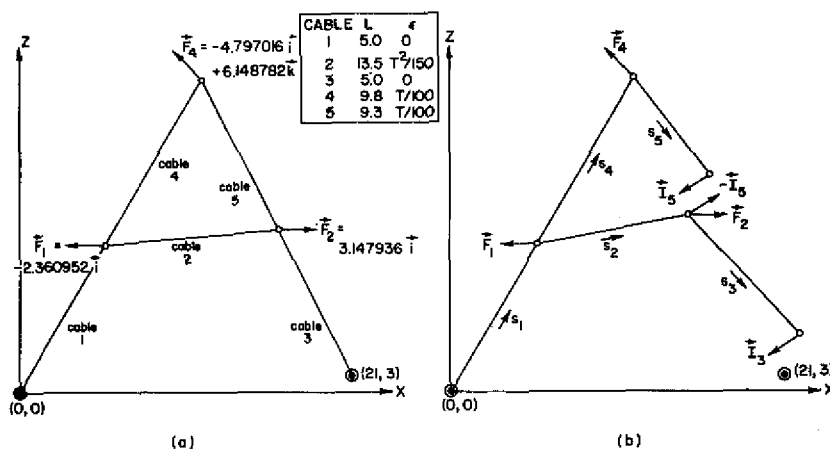


Fig. 5 - Example of the analysis of an internally redundant cable array by the Extended Method; (a) system of external loads and (b) decomposition of the array

and the strains are calculated from the appropriate cable constitutive relation. Finally the equilibrium configuration of the decomposed array is obtained from Eq. (3) as

$$P_1(s_1) = [R_1/T_1] s_1 ,$$

$$P_2(s_2) = P_1(L_1) + [1 + \epsilon_2] [R_2/T_2] s_2 ,$$

etc.

The error function E is defined by Eq. (4) as

$$E = \left\{ [21 - x_3(L_3)]^2 + [3 - z_3(L_3)]^2 + [x_2(L_2) - x_5(L_5)]^2 + [z_2(L_2) - z_5(L_5)]^2 \right\}^{1/2} ,$$

and the formulas for the changes in the imaginary reactions are given by Eq. (5) as

$$\Delta I_3 = (\delta/E) \{ [21 - x_3(L_3)] i + [3 - z_3(L_3)] k \}$$

and

$$\Delta I_5 = (\delta/E) \{ [x_2(L_2) - x_5(L_5)] i + [z_2(L_2) - z_5(L_5)] k \} .$$

The convergence of the extended method is demonstrated in Table 1 for a "good" initial guess and in Table 2 for a "bad" initial guess of the actual reactions. The parameter  $\delta$  is defined by  $\delta = 1/2^k$ . In both schemes the initial value of k was tried as -2. In Table 3, a comparison is made between the exact equilibrium configuration, from which the problem was derived, and the equilibrium configuration calculated during the final iteration in Table 1. Since the final value of E is less than  $5 \times 10^{-4}$ , the calculated coordinates are all known to be within  $\pm 0.0005$  of their true values. This fact is evident in Table 3.

Table 1  
Convergence of the Extended Method of Imaginary Reactions: "Good" Initial Guess

Iteration	$I_{3X}$	$I_{5X}$	$x_3(L_3)$	$x_2(L_2)$	$x_5(L_5)$	E	$\delta = 1/2^k$
	$I_{3Z}$	$I_{5Z}$	$z_3(L_3)$	$z_2(L_2)$	$z_5(L_5)$		k
0	5.000000 -4.000000	6.000000 -4.000000	19.911764 1.417750	16.007420 4.541225	15.293455 7.772219	$3.83 \times 10^0$	1
1	5.142223 -3.793214	6.093309 -4.422262	19.619953 5.383981	15.596247 8.352110	16.270474 6.638818	$3.31 \times 10^0$	2
2	5.246353 -3.973094	6.042436 -4.292988	20.335447 3.216381	16.349469 6.234987	16.196618 6.880840	$9.64 \times 10^{-1}$	2
3	5.418728 -4.029221	6.082083 -4.460513	20.644912 3.587505	16.632568 6.570976	16.894158 6.212847	$8.17 \times 10^{-1}$	3
4	5.473038 -4.119078	6.042074 -4.405738	20.938255 2.607824	16.943270 5.614500	16.818232 6.312403	$8.13 \times 10^{-1}$	4
5	5.477787 -4.088914	6.051691 -4.459416	20.873056 3.091175	16.866245 6.082073	16.917254 6.173390	$1.88 \times 10^{-1}$	4
6	5.519975 -4.119215	6.034739 -4.489764	20.990181 2.991145	16.982957 5.981488	16.988676 6.060209	$8.00 \times 10^{-2}$	7
7	5.520933 -4.118350	6.034181 -4.497449	20.986239 3.035169	16.978465 6.024775	16.999952 6.040205	$4.61 \times 10^{-2}$	7
8	5.523265 -4.124309	6.030540 -4.500063	20.999085 3.005318	16.992779 5.996890	16.999579 6.032894	$3.70 \times 10^{-2}$	8
9	5.523361 -4.124870	6.029823 -4.503861	20.997855 3.020894	16.991718 6.012694	17.004019 6.023381	$2.66 \times 10^{-2}$	8
10	5.523677 -4.127940	6.028015 -4.505431	21.002423 3.007859	16.997272 6.000979	17.003331 6.019728	$2.14 \times 10^{-2}$	8
11	5.523233 -4.129378	6.026907 -4.508861	21.001651 3.016341	16.997115 6.010284	17.005873 6.011742	$1.87 \times 10^{-2}$	9
...	...	...	...	...	...	...	...
31	5.518106 -4.138089	6.021677 -4.515889	21.000266 3.000355	17.000095 6.000127	17.000296 6.000304	$5.18 \times 10^{-4}$	13
32	5.518044 -4.138173	6.021630 -4.515931	21.000240 3.000087	17.000115 5.999920	17.000192 6.000272	$4.42 \times 10^{-4}$	

Table 2  
Convergence of the Extended Method of Imaginary Reactions: "Bad" Initial Guess

Iteration	$I_{3X}$	$I_{5X}$	$x_3(L_3)$	$x_2(L_2)$	$x_5(L_5)$	E	$\delta = 1/2^k$
	$I_{3Z}$	$I_{5Z}$	$z_3(L_3)$	$z_2(L_2)$	$z_5(L_5)$		k
0	-1.000000 2.000000	-2.000000 2.000000	10.193674 8.731501	12.429742 4.259365	-16.324218 19.345716	$3.47 \times 10^1$	-2
1	0.245725 1.339288	1.314681 0.260885	11.078499 15.828663	10.176189 10.910753	1.978978 15.541077	$1.88 \times 10^1$	-2
2	2.362064 -1.397173	3.063214 -0.726801	16.243958 -1.541930	11.940450 1.003618	4.540494 12.375103	$1.51 \times 10^1$	-1
3	2.992960 -0.794679	4.044829 -2.235246	15.504987 11.605196	10.672431 12.888318	5.659410 10.213462	$1.17 \times 10^1$	0
4	3.463238 -1.531136	4.473857 -2.006324	17.584443 5.967077	13.011434 7.988855	7.520010 11.149511	$7.79 \times 10^0$	0
5	3.901942 -1.912235	5.179191 -2.412288	17.730388 6.371451	13.240565 8.571791	9.819161 10.962750	$6.28 \times 10^0$	0
6	4.422308 -2.448809	5.723715 -2.792814	18.511665 5.077739	14.137512 7.499883	12.149437 10.406633	$4.79 \times 10^0$	0
7	4.941904 -2.882668	6.140103 -3.399780	19.093582 5.843562	14.774646 8.362846	14.512557 9.061670	$3.50 \times 10^0$	1
8	5.213946 -3.288439	6.177503 -3.499501	20.037657 3.281182	15.808536 5.948490	15.269935 8.649544	$2.93 \times 10^0$	2
9	5.296028 -3.312422	6.223443 -3.729885	20.022909 4.481649	15.783782 7.133027	15.738284 8.104645	$2.02 \times 10^0$	2
10	5.416723 -3.495442	6.229063 -3.849904	20.386960 3.807508	16.185753 6.518571	16.154257 7.713504	$1.57 \times 10^0$	2
11	5.514503 -3.624240	6.234086 -4.040496	20.582411 3.922167	16.404031 6.668280	16.604090 7.165600	$1.15 \times 10^0$	2
12	5.605642 -3.825502	6.190424 -4.149036	20.950299 3.068989	16.820354 5.887420	16.870855 6.794480	$9.12 \times 10^{-1}$	*

\*Clearly, the method is now converging to the equilibrium solution, as can be seen from iteration 2 or 3 in Table 1.

Table 3  
Comparison Between the Exact Equilibrium Configuration  
and That Calculated During the Final Iteration in Table 1

Cable	Exact			Calculated		
	$x_n(L_n)$	$z_n(L_n)$	$T_n$	$x_n(L_n)$	$z_n(L_n)$	$T_n$
1	3.000000	4.000000	2.513006	3.000070	3.999947	2.513294
2	17.000000	6.000000	2.671112	17.000115	5.999920	2.671196
3	21.000000	3.000000	6.897295	21.000240	3.000087	6.897339
4	9.000000	12.000000	2.040816	9.000007	12.000023	2.041049
5	17.000000	6.000000	7.526882	17.000192	6.000272	7.526863

#### Irrelevancy of the Location of the Internal Cut

Thus far the internally redundant cable array in Fig. 3 has been decomposed, in part, by making a cut above the junction of cables 3 and 5, and the point force  $F_2$  has been taken to act at the junction of cables 2 and 3 in the decomposed array. This situation is shown in Fig. 6a together with the chosen directions of increasing arc lengths. (The continuous loadings  $f_2(s_2)$  etc. have been suppressed for clarity.) However, this decomposition is not unique; actually the location of the internal cut and the disposition of the point loads are arbitrary in the solution of the equilibrium problem. Some other, but by no means all, possible decompositions of the internal loop are shown in Figs. 6b, 6c, and 6d.

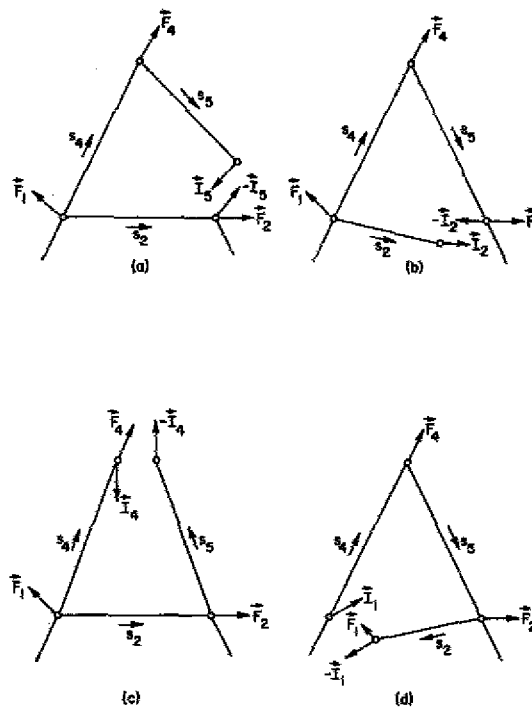


Fig. 6 - Some of the possible decompositions of the internal loop of cable

The values of the error function  $E$  and the additive internal reaction for these cases are as follows. For the case of Fig. 6b

$$E = \left\{ |A_3 - P_3(L_3)|^2 + |P_5(L_5) - P_2(L_2)|^2 \right\}^{1/2},$$

$$\Delta I_2 = (\delta/E) [P_5(L_5) - P_2(L_2)] ;$$

for the case of Fig. 6c

$$E = \left\{ |A_3 - P_3(L_3)|^2 + |P_5(L_5) - P_4(L_4)|^2 \right\}^{1/2},$$

$$\Delta I_4 = (\delta/E) [P_5(L_5) - P_4(L_4)] ;$$

and for the case of Fig. 6d

$$E = \left\{ |A_3 - P_3(L_3)|^2 + |P_2(L_2) - P_1(L_1)|^2 \right\}^{1/2},$$

$$\Delta I_1 = (\delta/E) [P_2(L_2) - P_1(L_1)] .$$

As previously, the additive reaction in each case is taken to act in the direction from its point of application to its required point of junction. Similarly, in each case, the iterative process to be followed in reducing the error function  $E$  to zero is exactly the same as outlined previously, with obvious modifications in the subscripting.

## GENERALIZATION TO ARBITRARY CABLE ARRAYS

### General Theory

Because of the infinite number of ways a cable array can be internally redundant, it becomes difficult to develop a simple and consistent notation for describing every possible array configuration. Rather, the generalization of the Extended Method to arbitrary cable arrays is best illustrated by example. To this end consider the problem of determining the equilibrium configuration of the system shown in Fig. 7. The array is loaded by a set of continuous forces  $f_1(s_1)$  etc. (which have been suppressed for clarity) and by a point force  $F$  acting at the apex.

The first step in the analysis is to make a sufficient number of cuts to render the array statically determinant and to replace the constraint released by each cut by a guessed reaction acting at the end of the cut (and for an internal cut by an equilibrating reaction acting at the opposite side of the cut). Application of this procedure to the system in Fig. 7 yields the decomposed array depicted in Fig. 8.

Since the array is now statically determinant, its equilibrium configuration under the loading of the guessed reactions can be easily calculated. For the decomposed array in Fig. 8, for example, the resultant force vectors are readily obtained by combining Eq. (1a) with a balance of forces at the cable junctions. When the directions of increasing arc length are taken as indicated in the figure, these vectors become

$$R_g(s_g) = I_g - \int_{L_g}^{s_g} f_g(\xi) d\xi, \quad (6a)$$

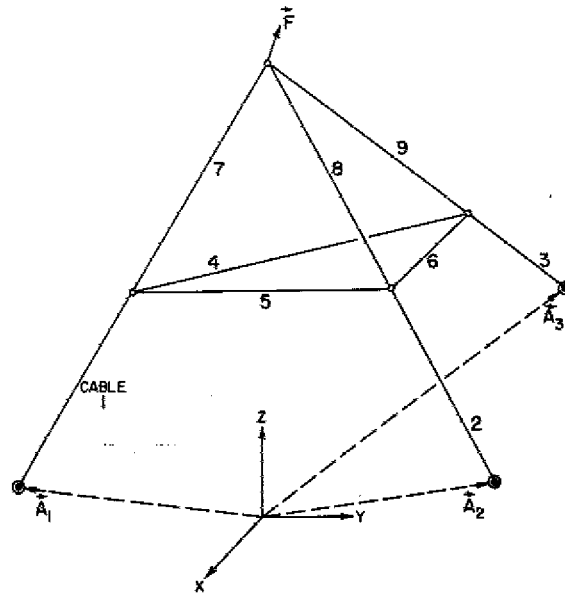


Fig. 7 - A multiply redundant cable array to be analyzed by the Extended Method

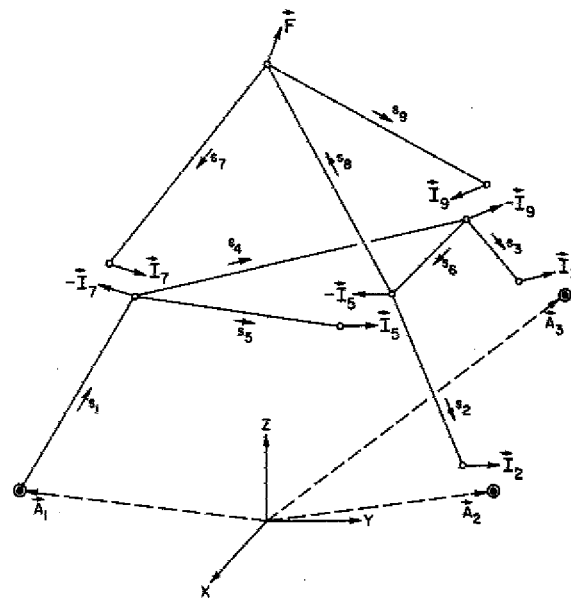


Fig. 8 - Decomposition of the cable array shown in Fig. 7 as prescribed by the Extended Method

$$R_7(s_7) = I_7 - \int_{L_7}^{s_7} f_7(\xi) d\xi, \quad (6b)$$

$$R_5(s_5) = I_5 - \int_{L_5}^{s_5} f_5(\xi) d\xi, \quad (6c)$$

$$R_3(s_3) = I_3 - \int_{L_3}^{s_3} f_3(\xi) d\xi, \quad (6d)$$

$$R_2(s_2) = I_2 - \int_{L_2}^{s_2} f_2(\xi) d\xi, \quad (6e)$$

$$R_8(s_8) = F + R_7(0) + R_9(0) - \int_{L_8}^{s_8} f_8(\xi) d\xi, \quad (6f)$$

$$R_6(s_6) = -I_5 + R_2(0) + R_8(0) - \int_{L_6}^{s_6} f_6(\xi) d\xi, \quad (6g)$$

$$R_4(s_4) = -I_9 + R_3(0) + R_6(0) - \int_{L_4}^{s_4} f_4(\xi) d\xi, \quad (6h)$$

$$R_1(s_1) = -I_7 + R_4(0) + R_5(0) - \int_{L_1}^{s_1} f_1(\xi) d\xi. \quad (6i)$$

The tensions  $T_n$ , strains  $\epsilon_n$ , and equilibrium coordinates  $P_n$  of the decomposed array can now be determined from Eqs. (1b), (1c), and (1d) respectively. This gives

$$P_1(s_1) = A_1 + \int_0^{s_1} [1 + \epsilon_1(\xi)] [R_1(\xi)/T_1(\xi)] d\xi, \quad (7a)$$

$$P_4(s_4) = P_1(L_1) + \int_0^{s_4} [1 + \epsilon_4(\xi)] [R_4(\xi)/T_4(\xi)] d\xi, \quad (7b)$$

$$P_6(s_6) = P_4(L_4) + \int_0^{s_6} [1 + \epsilon_6(\xi)] [R_6(\xi)/T_6(\xi)] d\xi, \quad (7c)$$

etc.

Again the basic problem is to find additive forces  $\Delta I_2$ ,  $\Delta I_3$ ,  $\Delta I_5$ ,  $(-\Delta I_5)$ ,  $\Delta I_7$ ,  $(-\Delta I_7)$ , and  $\Delta I_9$ ,  $(-\Delta I_9)$ , to be applied at the ends of cables 2, 3, 5, (6), 7, (1), and 9, (4), respectively, such that the decomposed array approaches its true equilibrium configuration. The Extended Method of Imaginary Reactions defines these forces as

$$\Delta I_2 = (\delta/E) [A_2 - P_2(L_2)] , \quad (8a)$$

$$\Delta I_3 = (\delta/E) [A_3 - P_3(L_3)] , \quad (8b)$$

$$\Delta I_5 = (\delta/E) [P_6(L_6) - P_5(L_5)] , \quad (8c)$$

$$\Delta I_7 = (\delta/E) [P_1(L_1) - P_7(L_7)] , \quad (8d)$$

$$\Delta I_9 = (\delta/E) [P_4(L_4) - P_9(L_9)] , \quad (8e)$$

where the error function  $E$  is again defined by the square root of the sum of the squares of the individual coordinate errors as

$$E = \left\{ |A_2 - P_2(L_2)|^2 + |A_3 - P_3(L_3)|^2 + |P_6(L_6) - P_5(L_5)|^2 + |P_1(L_1) - P_7(L_7)|^2 + |P_4(L_4) - P_9(L_9)|^2 \right\}^{1/2} \quad (9)$$

and where  $\delta$  is again a *positive* number chosen to guarantee convergence to the correct reactions.

As previously, each incremental reaction is taken to act in the direction from its point of application to its required point of junction, and  $E$  vanishes when and only when the correct equilibrium configuration has been obtained. The iterative procedure to be followed in reducing  $E$  to zero is exactly the same as the procedure developed previously and once again is globally convergent.

The technique for generalizing the Extended Method to other internally redundant arrays should by now be obvious.

#### Numerical Example II

To demonstrate the ability of the Extended Method to handle arbitrary cable arrays and the rapid convergence of the iterative process when the equilibrium calculations are programmed on a high-speed computer, a particular example concerning the multiply redundant array shown in Fig. 7 is considered.

The anchor points of the system are given (in feet) as

$$A_1 = -10000 \mathbf{i} ,$$

$$A_2 = 7000 \mathbf{i} - 7000 \mathbf{j} ,$$

$$A_3 = 7000 \mathbf{i} + 7000 \mathbf{j} + 1000 \mathbf{k} ,$$

and the unstressed cable lengths and constitutive relations are tabulated in Table 4. A plan view of the array is illustrated in Fig. 9.

The forces per unit of unstressed arc length are assumed identical for all cables in the array and taken (in lb/ft) as

$$\mathbf{f}_n(s_n) = d(\mathbf{i} \cos \theta + \mathbf{j} \sin \theta) - 0.03 \mathbf{k} ,$$

Table 4  
Cable Properties for Numerical Example II

Cable	L (ft)	$\epsilon$
1	11,300	$T/(6 \times 10^6)$
2	11,250	$T/(6 \times 10^6)$
3	10,550	$T/(6 \times 10^6)$
4	3,700	$T/(2 \times 10^6)$
5	3,700	$T/(2 \times 10^6)$
6	2,825	$T/(2 \times 10^6)$
7	3,100	$T/(4 \times 10^6)$
8	3,100	$T/(4 \times 10^6)$
9	3,100	$T/(4 \times 10^6)$

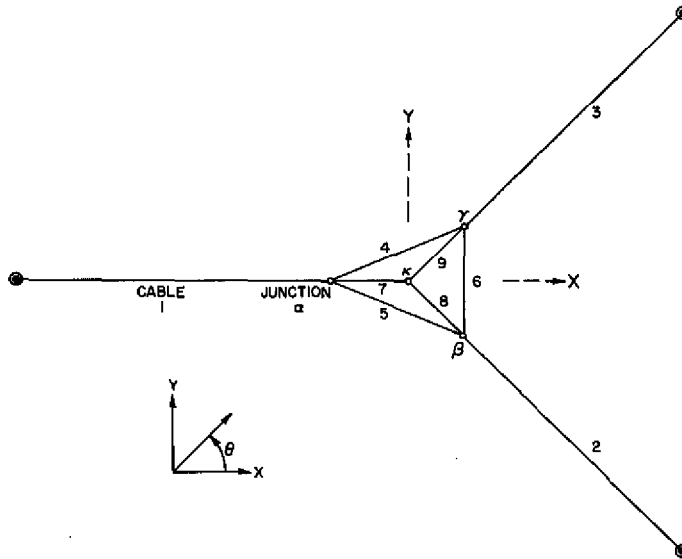


Fig. 9 - Plan view of the array considered in example II

where  $\theta$  (Fig. 9) represents the angle at which the horizontal component of load is applied to the array. The point load acting at the apex is given (in lb) by

$$F = D(i \cos \theta + j \sin \theta) + 20000 k .$$

When the array is decomposed as in Fig. 8, the resultant force vectors are readily obtained from Eq. (6), since

$$\int_{L_n}^{s_n} f_n(\xi) d\xi = [d(i \cos \theta + j \sin \theta) - 0.03 k](s_n - L_n) .$$

(For more complex loadings it is usually necessary or desirable to evaluate this integral numerically.) The tensions and strains are then calculated; finally, the equilibrium configuration of the decomposed array, under the influence of the guessed reactions, is determined by quadrature of Eq. (7). (For the particular loading and constitutive relations assumed in this example, the quadratures can be performed exactly. The algebra, though straightforward, is tedious and is not reproduced herein. For more complex situations a numerical determination of the equilibrium shape of the decomposed array is again usually necessary or desirable.) The guessed reactions are then varied in accordance with Eq. (8) until the calculated configuration of the decomposed array satisfies the geometric constraints imposed on the original array.

Two problems are considered. In the first the values of  $d$  and  $D$  are set equal to zero and the resulting shape of the array is found. In the second the values of  $d$  and  $D$  are taken as  $d = 0.05$  lb/ft and  $D = 125$  lb and the configuration of the system is determined for values of  $\theta$  from  $0^\circ$  to  $360^\circ$  in steps of  $10^\circ$ .

Typical results which can be obtained from the calculations are shown in Table 5 and Fig. 10. Table 5 gives the equilibrium locations of junctions  $\alpha$ ,  $\beta$ ,  $\gamma$ , and  $\kappa$  (defined in Fig. 9) for the case  $d = D = 0$ . Figure 10 depicts the  $X$ ,  $Y$ , and  $Z$  displacements of these junctions from their values in Table 5 when  $d$  and  $D$  assume their nonzero values.

Table 5  
Equilibrium Coordinates of Junctions  
 $\alpha$ ,  $\beta$ ,  $\gamma$ , and  $\kappa$  for the Case  $d = D = 0$

Junction	X (ft)	Y (ft)	Z (ft)
$\alpha$	-1984.3	38.0	7998.3
$\beta$	1434.5	-1373.1	8018.6
$\gamma$	1436.1	1450.6	8061.1
$\kappa$	-9.4	4.6	10398.8

For all cases examined the calculated configuration of the decomposed array was considered to have satisfied the geometric constraints imposed on the original array when the value of the error function became  $E \leq 0.1$ ; thus the equilibrium coordinates are accurate to within  $\pm 0.1$  ft. Run time, excluding compile, on the NRL/CDC 3800 computer averaged 30 seconds per case for the 37 cases considered, which nicely demonstrates the rapid convergence of the Extended Method.

#### STATICALLY UNSTABLE CABLE ARRAYS

Throughout this report the assumption that the cable array is statically stable (that is, under the action of the applied external loads no cable segment has zero tension) has been tacitly made. Of practical interest is the behavior of the technique of solution when this assumption proves false for the system under investigation. There are two cases to consider.

1. Suppose that the tension at one or more, but not all, of the anchor points approaches zero. The iterative process and consequently the equilibrium configuration of the array are not affected by this, and the solution simply reveals that these particular anchors are not necessary for the structural integrity of the system.

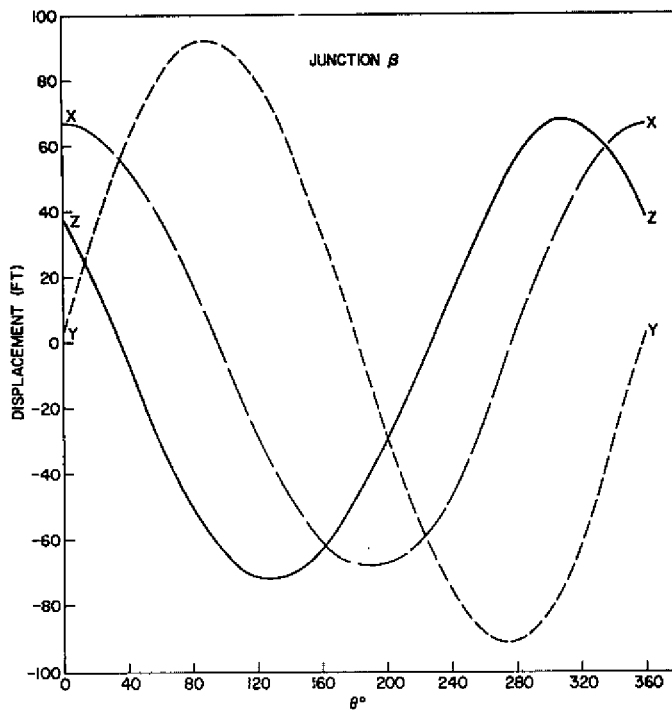
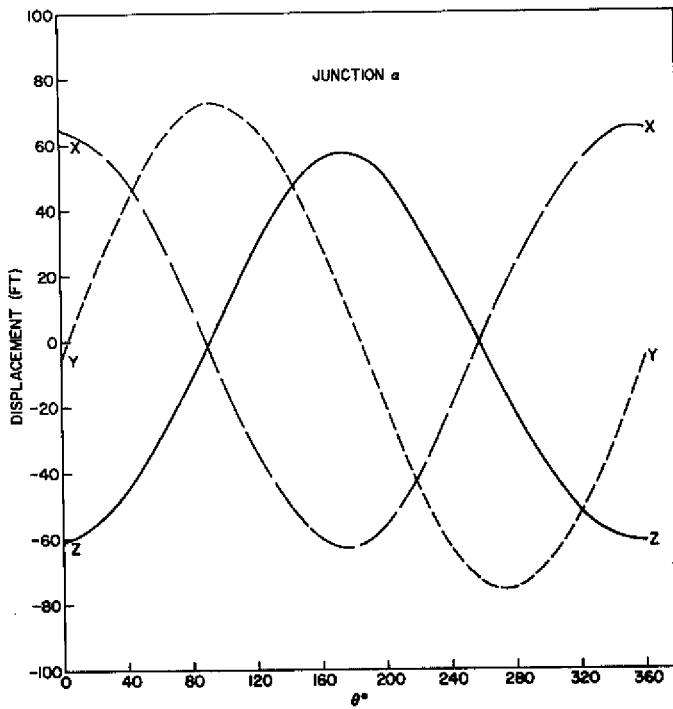


Fig. 10 - X, Y, and Z displacements of junctions  $\alpha$ ,  $\beta$ ,  $\gamma$ , and  $\kappa$  from their values in Table 5 when  $d$  and  $D$  assume their nonzero values

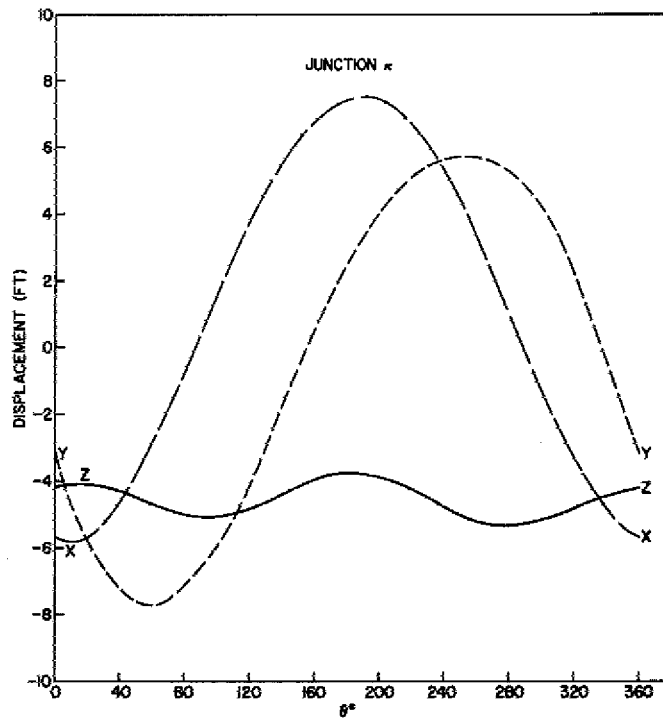
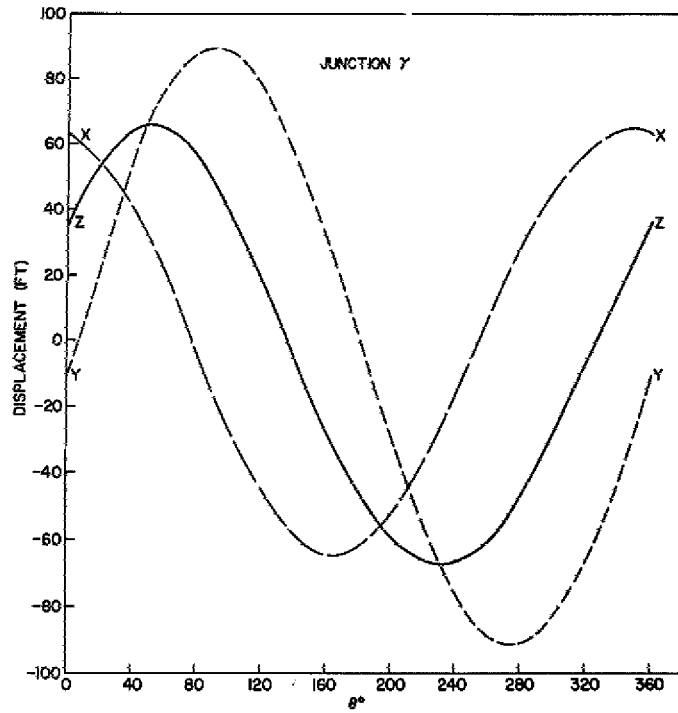


Fig. 10 (Continued) - x, y, and z displacements of junctions  $\alpha$ ,  $\beta$ ,  $\gamma$ , and  $\kappa$  from their values in Table 5 when  $d$  and  $D$  assume their nonzero values

2. Suppose that the tension at all anchor points or at one or more internal segments of the array approaches zero. Then, as is shown in the second (concluding) section of the Appendix, the change  $dE$  in  $E$  approaches  $-\infty$ . As a result it becomes impossible to find a  $\delta$  such that  $E' < E$ ; consequently

$$\lim_{\delta \rightarrow 0} E = \text{constant} \neq 0 .$$

Thus the calculated configuration must be incorrect. However, it is self-consistent in the sense that an examination of the generated solution reveals those segments, and only those segments, in which the tension is actually zero under the applied loads. To proceed, it is now possible to remove the zero-tension segments from the array and to solve for the equilibrium configuration of the modified array.

These properties of the Extended Method to identify slack line segments of the array during the course of the analysis are useful in that they make a preliminary stability investigation of the system unnecessary.

### CONFIGURATION-DEPENDENT EXTERNAL FORCES

Thus far it has been assumed that the point loads  $F_n$  acting on a cable array are known numbers and that the continuous loads  $f_n$  are known functions of the unstressed arc lengths  $s_n$ . In many applications, especially those involving the calculation of mooring motions under hydrodynamic forces, this assumption fails to hold, and the external loads become dependent on the configuration of the array. That is, the  $F_n$  become functions of the location in space of their point of application, and the  $f_n$  become functions not only of  $s_n$  but also of  $P_n(s_n)$  and  $dP_n/ds_n$ .

Under a large class of these configuration-dependent loads, however, the equilibrium shape of the array can still be determined by combining the Extended Method with the mathematical technique of successive approximations (4). This technique is briefly described.

Suppose that in Fig. 3 the point and continuous loads are functions of the configuration of the array. Make an initial estimate of the final array configuration (this estimate need not be very accurate), and from this configuration calculate the estimated values of  $F_n$  and the estimated functional relations  $f_n(s_n)$ . Or, even more simply, just make an educated guess at the values of  $F_n$  and the relations  $f_n(s_n)$ . Note, these initial estimates are used only for starting the successive approximation routine; from here on the routine is automatic.

With the estimated loads employed, calculate the equilibrium shape of the array by using the Extended Method. After this position is determined, make corrected estimates of the external loads, and find a corrected equilibrium shape. This process is repeated until the equilibrium configuration has been obtained to within a specified accuracy and converges under certain conditions of continuity and boundedness of the external forces (4).

This combined technique has previously been used in Ref. 5 for the analysis of the current-induced motions of  $N$ -point moors by the Method of Imaginary Reactions. This reference gives a detailed description of the technique and its applications.

## CONCLUSIONS

The method presented in this report is applicable to the analysis of a wide range of internally redundant cable systems including suspension bridges, structural nets, and moorings. The method itself involves no more than elementary statics once the external force distribution has been defined and should prove particularly attractive to the practicing engineer who would otherwise be faced with the simultaneous solution of large, interdependent sets of force-balance, geometric-constraint equations which are grossly nonlinear.

The iterative procedure which characterizes the technique is unique in that it is globally convergent to the equilibrium configuration of the array and does not require the calculation of any slopes or derivatives. This latter property results in considerable savings of time and storage on the computer.

Although the static stability of the cable system is assumed, situations in which slack line segments arise are identified in the course of the analysis. Thus preliminary stability investigations are unnecessary.

External loads are also assumed to be independent of the array configuration. However, when this assumption does not hold, the equilibrium configuration of the array can still be determined by combining the method of solution with the mathematical technique of successive approximations. This combined technique is particularly important in the analysis of mooring systems.

## REFERENCES

1. Skop, R.A., and O'Hara, G.J., "The Static Equilibrium Configuration of Cable Arrays by Use of the Method of Imaginary Reactions," NRL Report 6819, Feb. 28, 1969
2. Skop, R.A., and O'Hara, G.J., "The Method of Imaginary Reactions - A New Technique for Analyzing Structural Cable Systems," Marine Technology Soc. J. 4 (No. 1), 21-30 (Jan./Feb. 1970)
3. Pahuja, S.C., "Modeling and Analysis of a Tri-Moored Buoy Structure with One Tie-Leg," M.S. Dissertation, University of New Hampshire, June 1970
4. Burkill, J.C., "The Theory of Ordinary Differential Equations," Chapter I, Interscience, New York, 1962
5. Skop, R.A., "The Method of Imaginary Reactions: Applications to  $N$ -Point Moors," Marine Technology 1970, Preprints of 6th Annual Marine Technology Society Conference, Vol. 1, pp. 1-22, June 29 - July 1, 1970, Washington, D.C.

## Appendix

### PROOF OF THE CONVERGENCE AND THE UNIQUENESS OF THE EXTENDED METHOD OF IMAGINARY REACTIONS

#### STATICALLY STABLE ARRAYS

In this appendix the proof is given that the Extended Method of Imaginary Reactions converges to the unique equilibrium configuration of an internally redundant cable array from any set of initially guessed reactions consistent with the static stability of the array.

To facilitate this proof, it is expedient to introduce some additional notation. Let those cables in an array which are released from anchor points and to which external guessed reactions are applied at  $s = L$  be denoted by the set of subscripts  $\{r_1, r_2, \dots, r_M\}$ . Further, let those cables to which internal guessed reactions are applied at  $s = L$  be given by the subscripts  $\{i_1, i_2, \dots, i_N\}$ , and let those cables to which the corresponding equilibrating reactions are applied at  $s = L$  be represented by the subscripts  $\{e_1, e_2, \dots, e_N\}$ . Thus, for the decomposed array in Fig. 4,  $\{r\} = \{3\}$ ,  $\{i\} = \{5\}$ , and  $\{e\} = \{2\}$ ; and for the decomposed array in Fig. 8,  $\{r\} = \{2, 3\}$ ,  $\{i\} = \{5, 7, 9\}$ , and  $\{e\} = \{6, 1, 4\}$ .

In terms of this notation the error function  $E$ , defined as the square root of the sum of the squares of the individual coordinate errors, can be written in matrix form as

$$E^2 = D^T D, \quad (A1a)$$

where the column matrix  $D$  of individual coordinate differences is given by

$$D = \begin{bmatrix} A_{r_1} - P_{r_1}(L_{r_1}) \\ \vdots \\ A_{r_M} - P_{r_M}(L_{r_M}) \\ P_{e_1}(L_{e_1}) - P_{i_1}(L_{i_1}) \\ \vdots \\ P_{e_N}(L_{e_N}) - P_{i_N}(L_{i_N}) \end{bmatrix} \quad (A1b)$$

and where the matrix  $D^T$  represents the transpose of  $D$ .

Consider now the total differential of Eq. (A1a). Since, for a statically determinant array, the equilibrium coordinates are functions of *only* the guessed reactions  $I_{r_1}, I_{r_2}, \dots$  and  $I_{i_1}, I_{i_2}, \dots$  applied at the ends of cables  $r_1, r_2, \dots$  and  $i_1, i_2, \dots$  respectively, this differential is

$$E dE = -D^T J dI, \quad (\text{A2a})$$

where  $I$ , the column matrix of guessed reactions, is defined by

$$I = \begin{bmatrix} I_{r_1} \\ \vdots \\ I_{r_M} \\ I_{i_1} \\ \vdots \\ I_{i_N} \end{bmatrix} \quad (\text{A2b})$$

The square matrix  $J$  is equal to the Jacobian matrix of the transformation from "end-coordinate error" space to "imaginary reaction" space. This matrix is conveniently written as

$$J = [\partial(-D^T)/\partial(I^T)], \quad (\text{A2c})$$

where the notation implies that the  $ij$ th element of  $J$  is obtained by taking the partial derivative of the  $i$ th element of  $-D^T$  with respect to the  $j$ th element of  $I^T$ .

On recalling that the Extended Method of Imaginary Reactions defines  $dI$  as

$$dI = (\delta/E) D, \quad (\text{A3})$$

Eq. (A2a) for the total differential of  $E$  can be recast as

$$dE = -(\delta/E^2) Q, \quad (\text{A4a})$$

where  $Q$  is the quadratic form

$$Q = D^T J D. \quad (\text{A4b})$$

If it can now be shown that  $Q$  is positive definite, vanishing only at  $D = 0$  (where  $0$  is the null matrix), the convergence of the Extended Method to a unique set of equilibrium reactions (and, consequently, to the unique equilibrium configuration of the cable array) follows from the argument given in the next paragraph.

Suppose  $Q$  is positive definite. Then the Jacobian,  $\det J$ , of the transformation from end-coordinate error space to imaginary reaction space is *positive*.\* Thus, the transform is one-to-one†; that is, a unique set of end-coordinate errors determines a

\*R.A. Frazer, W.J. Duncan, and A.R. Collar, "Elementary Matrices," Chapter I, New York: Macmillan, 1947.

†A.E. Taylor, "Advanced Calculus," Chapter IX, Boston: Ginn, 1955.

unique set of reactions and vice versa. In particular the equilibrium set of errors  $D = 0$  determines the unique set of reactions for which  $E = 0$ . Further, the Extended Method converges to this set of reactions from any set of initially guessed reactions. For, if  $Q$  is positive definite, then  $dE$ , defined by Eq. (A4a), is negative definite for  $\delta$  greater than zero. Thus the existence of a *positive*  $\delta$  which makes  $E' < E$  follows from the Mean Value Theorem; and since  $E = 0$  at only one point in reaction space, global convergence of the iterative process to this point is guaranteed.

Therefore it remains only to show that  $Q$  is indeed positive definite. To this end, certain preliminary calculations are necessary. Note first that in a decomposed array the resultant force in any cable located on a path between the point of application of a guessed reaction and the fixed (anchor) point of the array contains this reaction in a linear manner. For example, for the array in Fig. 4

$$\begin{aligned} R_1(s_1) &= I_3 + G_1(s_1) , \\ R_2(s_2) &= I_3 - I_5 + G_2(s_2) , \\ R_4(s_4) &= I_5 + G_4(s_4) , \end{aligned}$$

etc., and for the array in Fig. 8

$$\begin{aligned} R_8(s_8) &= I_7 + I_9 + G_8(s_8) , \\ R_6(s_6) &= I_2 - I_5 + I_7 + I_9 + G_6(s_6) , \end{aligned}$$

etc. In these expressions the  $G_n$  terms are functions of the applied external loads but are *independent of the guessed reactions*.

The next preliminary calculation is finding the partial derivative of

$$H_n = \int_0^{L_n} [1 + \varepsilon_n(\xi)] [R_n(\xi)/T_n(\xi)] d\xi \quad (A5)$$

with respect to the guessed reaction  $I_k$ . By using the facts that the resultant force vectors contain only linear combination of the guessed reactions, that  $T_n = |R_n|$ , and that  $\varepsilon_n = \varepsilon_n(T_n, s_n)$ , this derivative becomes

$$\partial H_n / \partial I_k = \int_0^{L_n} [\text{sgn}_n(I_k)] B_n(\xi) d\xi . \quad (A6a)$$

Here  $B_n$  is a square matrix given by

$$B_n(s_n) = \begin{bmatrix} B_{nXX} & B_{nXY} & B_{nXZ} \\ B_{nYX} & B_{nYY} & B_{nYZ} \\ B_{nZX} & B_{nZY} & B_{nZZ} \end{bmatrix} , \quad (A6b)$$

and the function  $\text{sgn}_n(I_k)$  is defined as

$$\text{sgn}_n(I_k) = \begin{cases} +1 & \text{if } R_n \text{ depends on } +I_k, \\ 0 & \text{if } R_n \text{ is independent of } I_k, \\ -1 & \text{if } R_n \text{ depends on } -I_k. \end{cases} \quad (\text{A6c})$$

The individual elements  $B_{nab}$  of  $B_n$  are readily calculated as

$$B_{nab}(s_n) = \frac{R_{na}R_{nb}}{T_n} \frac{d}{dT_n} \left( \frac{1 + \epsilon_n}{T_n} \right) + \left( \frac{1 + \epsilon_n}{T_n} \right) \delta_{ab}, \quad (\text{A6d})$$

where  $\delta_{ab}$  is the Kronecker delta:

$$\delta_{ab} = \begin{cases} 1 & \text{if } a = b, \\ 0 & \text{if } a \neq b. \end{cases}$$

On expanding the derivative in Eq. (A6d),  $B_{nab}$  can be recast as

$$B_{nab} = \frac{1}{T_n^2} \frac{d\epsilon_n}{dT_n} R_{na}R_{nb} + \frac{(1 + \epsilon_n)}{T_n^3} (T_n^2 \delta_{ab} - R_{na}R_{nb}). \quad (\text{A6e})$$

As a final preliminary calculation, consider the matrix  $B_n$ . By substituting Eq. (A6e) into Eq. (A6b),  $B_n$  can easily be shown to have the form

$$B_n(s_n) = R_n^T R_n + S_n^T S_n, \quad (\text{A7a})$$

where  $R_n$  is the row matrix

$$R_n(s_n) = \left( \frac{1}{T_n^2} \frac{d\epsilon_n}{dT_n} \right)^{1/2} [R_{nX} \quad R_{nY} \quad R_{nZ}] \quad (\text{A7b})$$

and where  $S_n$  is the square matrix

$$S_n(s_n) = \left( \frac{1 + \epsilon_n}{T_n^3} \right)^{1/2} \begin{bmatrix} 0 & -R_{nZ} & R_{nY} \\ R_{nZ} & 0 & -R_{nX} \\ -R_{nY} & R_{nX} & 0 \end{bmatrix}. \quad (\text{A7c})$$

Both of these matrices are real, since physically, for a perfectly flexible cable, the quantities  $T_n$ ,  $\epsilon_n$ , and  $d\epsilon_n/dT_n$  must all be positive.

Consider now the manner in which an end coordinate of a decomposed cable array is determined. By referring to the equilibrium equations (3) and/or (7), it becomes apparent that this coordinate is obtained as a summation over a certain set of cables of the integrals  $H_n$ , given by Eq. (A5). Thus, the end-coordinate error matrix  $D$ , Eq. (A1b), can always be decomposed into a summation over the individual cables in an array as

$$\lim_{\delta \rightarrow 0} E = \text{constant} \neq 0 .$$

As is remarked in the main text, the above result is thus indicative of a statically unstable cable array.